

## Werk

**Jahr:** 1977

**Kollektion:** fid.geo

**Signatur:** 8 Z NAT 2148:44

**Digitalisiert:** Niedersächsische Staats- und Universitätsbibliothek Göttingen

**Werk Id:** PPN1015067948\_0044

**PURL:** [http://resolver.sub.uni-goettingen.de/purl?PPN1015067948\\_0044](http://resolver.sub.uni-goettingen.de/purl?PPN1015067948_0044)

**LOG Id:** LOG\_0089

**LOG Titel:** Crustal structure of the Rhenish massif and adjacent areas; a reinterpretation of existing seismic-refraction data

**LOG Typ:** article

## Übergeordnetes Werk

**Werk Id:** PPN1015067948

**PURL:** <http://resolver.sub.uni-goettingen.de/purl?PPN1015067948>

**OPAC:** <http://opac.sub.uni-goettingen.de/DB=1/PPN?PPN=1015067948>

## Terms and Conditions

The Goettingen State and University Library provides access to digitized documents strictly for noncommercial educational, research and private purposes and makes no warranty with regard to their use for other purposes. Some of our collections are protected by copyright. Publication and/or broadcast in any form (including electronic) requires prior written permission from the Goettingen State- and University Library.

Each copy of any part of this document must contain these Terms and Conditions. With the usage of the library's online system to access or download a digitized document you accept the Terms and Conditions.

Reproductions of material on the web site may not be made for or donated to other repositories, nor may be further reproduced without written permission from the Goettingen State- and University Library.

For reproduction requests and permissions, please contact us. If citing materials, please give proper attribution of the source.

## Contact

Niedersächsische Staats- und Universitätsbibliothek Göttingen  
Georg-August-Universität Göttingen  
Platz der Göttinger Sieben 1  
37073 Göttingen  
Germany  
Email: [gdz@sub.uni-goettingen.de](mailto:gdz@sub.uni-goettingen.de)

## **Crustal Structure of the Rhenish Massif and Adjacent Areas; a Reinterpretation of Existing Seismic-Refraction Data\***

W.D. Mooney\*\*

Geophysical and Polar Research Center, University of Wisconsin, Madison, WI 53706, USA

C. Prodehl

Geophysikalisches Institut der Universität, Hertzstr. 16, D-7500 Karlsruhe 21,  
Federal Republic of Germany

**Abstract.** Most of the existing seismic-refraction profiles in the Rhenish Massif/Rhenohercynian zone of Western Germany have been jointly reinterpreted using traveltime and amplitude information. The general pattern of observed phases can be divided into three types; each type corresponds to a distinct kind of velocity structure.

Type I: Throughout the central Rhenish Massif and the adjacent Hessische Senke a strong P-phase reflection from the crust-mantle boundary is recorded in regions where no major volcanic features are crossed by the lines of seismic observations. The average crustal thickness is 28–29 km, the average crustal velocity (excepting sediments) is 6.2–6.3 km/sec, and the crust is nearly homogeneous. This structure is here referred to as the Rhenohercynian crustal model.

Type II: Beneath the southern part of the Rhenish Massif and two areas in the northeast and southeast some structure within the crust is evident. Both an intracrustal and the Moho discontinuities are evidenced by strong reflected phases, the Moho reflection being the stronger one. Along the profiles crossing major volcanic features such as Vogelsberg and central Westerwald, but not beneath the eastern Eifel, the M-discontinuity is heavily disrupted or “smeared” and an intermediate intracrustal boundary at about 20 km depth forms the main reflector for seismic waves. Beneath this boundary the velocity increases gradually from about 7 km/sec to upper-mantle velocities.

Type III: For profiles crossing the northern Rhine Graben area as well as for a line from the Siebengebirge through the Rhenish Massif to the north, east of the Lower Rhine basin, the observed phases indicate only one major seismic boundary at a depth of about 23 km where the velocity

---

\* Contribution within the priority research program of the Deutsche Forschungsgemeinschaft “The driving mechanism of epirogenic movements: Rhenish shield”

Contribution no. 153 Geophysical Institute, University of Karlsruhe

\*\* also Geophysikalisches Institut der Universität Karlsruhe

increases rapidly to 7.3 km/sec. Below this boundary the velocity increases gradually with depth reaching 8 km/sec at 27–28 km.

The occurrence of types I, II, and III can be roughly correlated with tectonic setting. The  $P_n$  phase is recorded with variable success and disappears completely on a profile passing the eastern Eifel volcanics, but is clear on the lines through Vogelsberg and central Westerwald. The petrographic differences between these volcanics appear such to be reflected in the behaviour of the seismic waves. Cross sections and areal views are used to display the variations in crustal and upper mantle velocity structure.

**Key words:** Seismic-refraction profiles – Crustal structure – Lateral variations – Rhenish Massif – Rhenohercynian zone.

## Introduction

The Rhenish Massif is part of the Variscan mountain system of western Europe and as such part of the Rhenohercynian zone being located as a consolidated block between the Upper Rhine Graben in the south, the Lower Rhine Basin in the northwest, and the Hessische Senke in the east. Tertiary to Quarternary volcanism is concentrated in the Westerwald, Eifel and Siebengebirge and the adjacent Hessische Senke to the east. Since the Mesozoic the Rhenish Massif has been undergoing uplift, a movement which seems still to be active today. Within the scope of a priority program, sponsored by the German Research Society, aimed at the investigation of vertical movements and their origin, the

**Table 1.** Profiles observed in the area of the Rhenohercynian zone and reinterpreted in this report with number of recordings (up to January 1971) and references

N1 = Number of explosions which were used for the corresponding profile. N2 = Number of photographic records. N3 = Number of magnetic-tape records

Profile	N1	N2	N3	
02-165-01	10	52	21	German Research Group, 1964; Fuchs and Landisman, 1966a, b; Ansorge et al., 1970; Wangemann, 1970; Fuchs and Müller, 1971; Giese and Stein, 1971; Bamford, 1973; Mueller et al., 1973; Giese, 1976a, b; Müller and Fuchs, 1976; Mooney and Prodehl, 1977
02-215	04	33	16	Meissner and Berckhemer, 1967; Mueller et al., 1969; Wilde, 1969; Meissner et al., 1970; Giese and Stein, 1971; Bamford, 1973; Mueller et al., 1973; Meissner and Vetter, 1974; Rhine-Graben Research Group 1974; Giese, 1976a, b; Meissner et al., 1976a; Mooney and Prodehl, 1977
02-220-05	02	17	00	Strobach, 1963; German Research Group, 1964; Giese and Stein, 1971; Bamford, 1973; Meissner and Vetter, 1974; Rhine-Graben Research Group, 1974; Giese, 1976a, b; Meissner et al., 1976a; Prodehl et al., 1976; Mooney and Prodehl, 1977

**Table 1** (continued)

Profile	N1	N2	N3	
02-265	05	39	00	Behnke, 1961 a; Closs and Behnke, 1961; German Research Group, 1964; Hänel, 1964; Giese and Stein, 1971; Bamford, 1973, 1976 a, b; Giese, 1976 a, b; Mooney and Prodehl, 1977
02-350-06	07	19	22	German Research Group, 1964; Fuchs and Landisman, 1966 a, b; Wangemann, 1970; Giese and Stein, 1971; Bamford, 1973; Giese, 1976 a, b; Mooney and Prodehl, 1977
03-250	02	37	00	Hänel, 1963; German Research Group, 1964; Hänel, 1964; Giese and Stein, 1971, Bamford, 1973; Meissner and Vetter, 1974; Bamford, 1976 a, b; Meissner et al., 1976 b; Giese, 1976 a, Mooney and Prodehl, 1977
06-170-20	04	45	08	German Research Group, 1964; Fuchs and Landisman, 1966 a, b; Wangemann, 1970; Giese and Stein, 1971; Bamford, 1973; Giese, 1976 a, b; Mooney and Prodehl, 1977
06-260	04	23	11	Closs and Behnke, 1961; Plaumann, 1961 a; German Research Group, 1964; Giese and Stein, 1971, Bamford, 1973, 1976 a, b; Giese, 1976 a, b; Mooney and Prodehl, 1977
08-000	01	20	00	Plaumann, 1961 b; Hänel, 1963; German Research Group, 1964; Giese and Stein, 1971, Giese, 1976 a; Prodehl et al., 1976; Mooney and Prodehl, 1977
12-260	03	30	06	Hänel, 1963; German Research Group, 1964; Hänel, 1964; Giese and Stein, 1971; Bamford, 1973; Meissner and Vetter, 1974; Bamford, 1976 a, b; Giese, 1976 a; Meissner et al., 1976 b; Mooney and Prodehl, 1977
13-120-09	05	53	20	Stein, 1963; German Research Group, 1964; Giese and Stein, 1971; Bamford, 1973; Mooney and Prodehl, 1977
13-240-20	03	00	55	Giese and Stein, 1971; Bamford, 1973, 1976 a, b; Mooney and Prodehl, 1977
14-010	05	13	34	Giese and Stein, 1971, Thyssen et al., 1971; Giese, 1976 b; Mooney and Prodehl, 1977
14-090-02	02	36	00	German Research Group, 1964; Giese and Stein, 1971; Bamford, 1973, 1976 a, b; Giese, 1976 a, b; Mooney and Prodehl, 1977
16-080	02	19	09	Meissner and Berckhemer, 1967; Meissner et al., 1970; Giese and Stein, 1971; Bamford, 1973; Meissner and Vetter, 1974; Rhine-Graben Research Group, 1974; Giese, 1976 a; Meissner et al., 1976 b; Prodehl et al., 1976; Mooney and Prodehl, 1977
17-240-20	05	00	95	Giese and Stein, 1971; Giese, 1976 a; Mooney and Prodehl, 1977
20-070-22	05	00	59	Giese and Stein, 1971; Weber, 1973; Giese, 1976 a; Mooney and Prodehl, 1977
22-060-17	02	00	13	Mooney and Prodehl, 1977
240-LO-060	8	00	173	Bartelsen, 1970; Giese and Stein, 1971; Meissner and Vetter, 1974; Giese, 1976 a; Glocke and Meissner, 1976; Meissner et al., 1976 a, b; Mooney and Prodehl, 1977

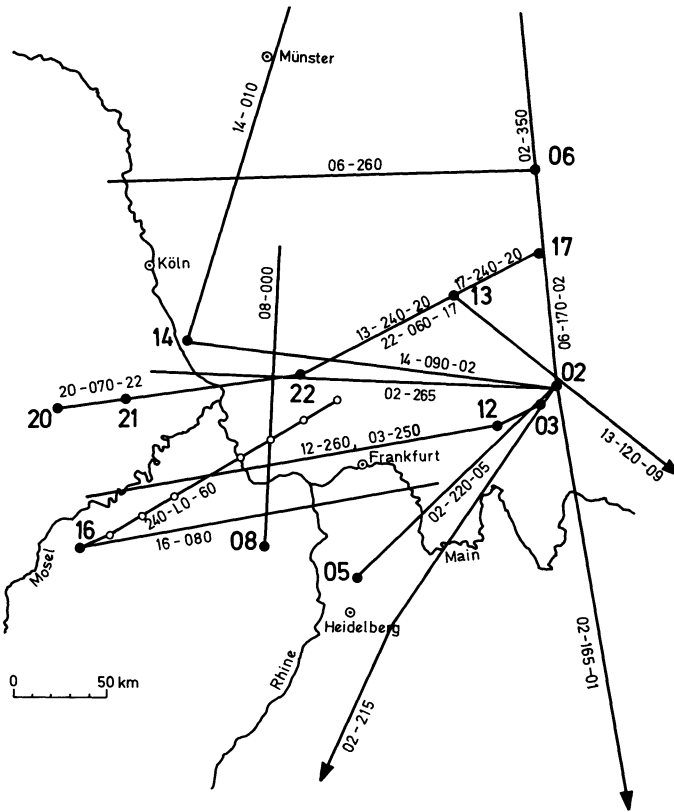


Fig. 1. Location map of seismic-refraction profiles in the Rhenohercynian zone.

*Explanation:* ●— profiles. 16-080-02 shotpoint code—azimuth—reversed shotpoint code. 12-240 shotpoint code—azimuth—(no reversed shot). ○— common-depth point profile. 240-LO-060 with center near LO=Loreley. Shotpoints: 02 Hilders, 03 Gersfeld, 05 Birkenau, 06 Adelebsen, 08 Kirchheimbolanden, 12 Roms-thal, 13 Dorheim, 14 Mehrberg, 15 Büdingen, 16 Taben Rodt, 17 Bransrode, 20 Birresborn, 21 Bermel, 22 Dorndorf

Rhenish Massif is at present being investigated in detail in a broad-scale geoscientific effort.

Within two former priority programs of the German Research Society: The Deep Structure of Central Europe (1958–1964) and Upper Mantle Project (1965–1974), explosion seismology investigations of central Europe were based mainly on quarry blast observations. A part of these programs covered also the Rhenohercynian zone where numerous quarries firing large explosions are located. These programs are described in general by Giese, Prodehl and Stein (1976); publications dealing with individual profiles are listed in Table 1. This paper concentrates on the reinterpretation of profiles obtained within the area of the Rhenohercynian zone during the two former priority programs mentioned above. Figure 1 shows the quarries used as shotpoints and the corresponding profiles, while Figure 2 shows the geologic position of these quarry blast observa-

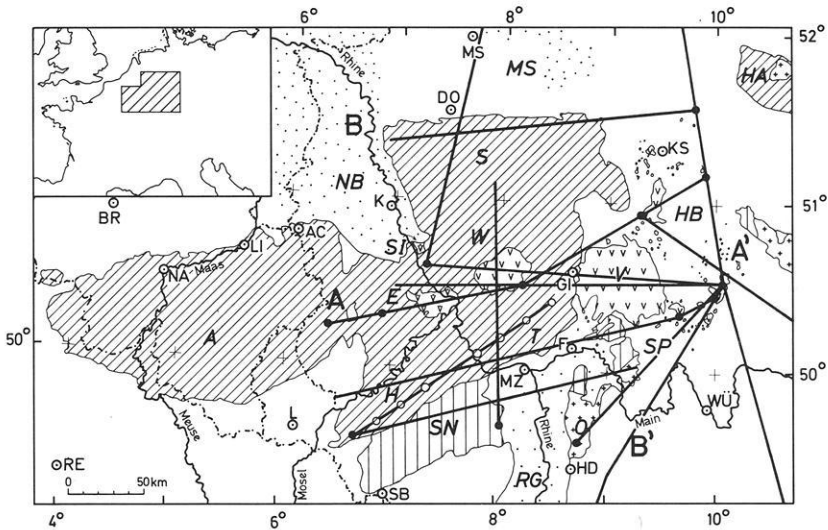


Fig. 2. Location of seismic-refraction profiles on a generalized geologic map of the Rhenohercynian zone and adjacent areas.

*Explanation:* [stippled] Quaternary and Tertiary, [white] Mesozoic, [vertical lines] Permian, [diagonal lines] Carboniferous and Devonian, [inverted triangles] Trachytes and phonolites, [triangles] Young Tertiary volcanics, [dots] Plutonites, [solid line with arrow] Shotpoints and recording lines, [line with circles] Common-depth point profile, **AA'** Location of cross section of Figure 17, **BB'** Location of cross section of Figure 18.

○ Cities: AC Aachen, DO Dortmund, LI Liège, KS Kassel, L Luxembourg, F Frankfurt, BR Bruxelles, K Köln, GI Gießen, SB Saarbrücken, HD Heidelberg, NA Namur, MS Münster, MZ Mainz, WÜ Würzburg.

*A* Ardennes, *E* Eifel, *H* Hunsrück, *HA* Harz, *HB* Hessische Senke, *MS* Münsterländer Bucht, *N* Neuwieder Becken, *NB* Niederrheinische Bucht, (Lower Rhine Basin), *O* Odenwald, *RG* Rhine Graben, *S* Sauerland, *SI* Siebengebirge, *N* Saar-Nehe trough, *SP* Spessart, *T* Taunus, *V* Vogelsberg, *W* Westerwald

tions. It can be noted that only a few of the profiles run entirely in the Rhenish Massif proper but partly cross the volcanic areas within and east of the Rhenish Massif. As the quarries with usable blasts are spread more or less randomly, the normal requirement of seismic-refraction measurements of having reverse and overlapping profiles could only be fulfilled by one special line running from Birresborn in the Eifel (shotpoint 20 on Figs. 1 and 2) to Bransrode (no. 17) in the Rhön, which was initiated and organized by Stein (1977). Also, the position of the profiles is not always optimal with regard to geologic and tectonic settings of the area.

In spite of these complications the record sections of the numerous profiles exhibit a similar pattern of travelt ime branches which permit a classification of the observed record sections in relation to its geologic and tectonic situation. Conventional flat-layer methods of interpretation using trial and error fitting of traveltimes and amplitudes have been applied with care.

For some profiles the data clearly show that lateral heterogeneities play a major role. We have, however, produced for all profiles flat-layer approximations of the velocity-depth structure. On the other hand, the variable quality

of the available data and the infrequency of reversing and overlapping profiles does not justify the use of a more sophisticated method which would take care of lateral inhomogeneities in particular.

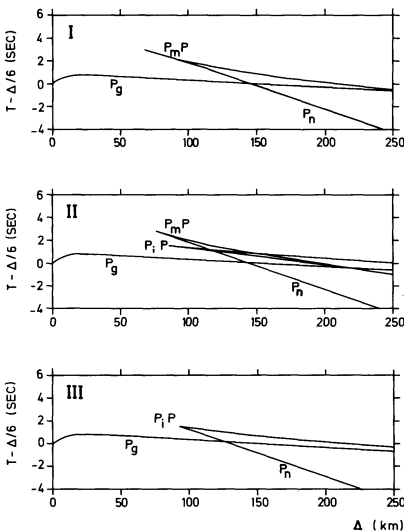
### Correlation and Inversion of Phases

As a first step in the correlation we have identified the wave penetrating into the basement,  $P_g$ , the Moho reflection,  $P_mP$ , and the mantle "head" or diving wave,  $P_n$ . In some cases other phases are apparent, while in still other cases  $P_mP$  or  $P_n$  are either weak or completely missing.

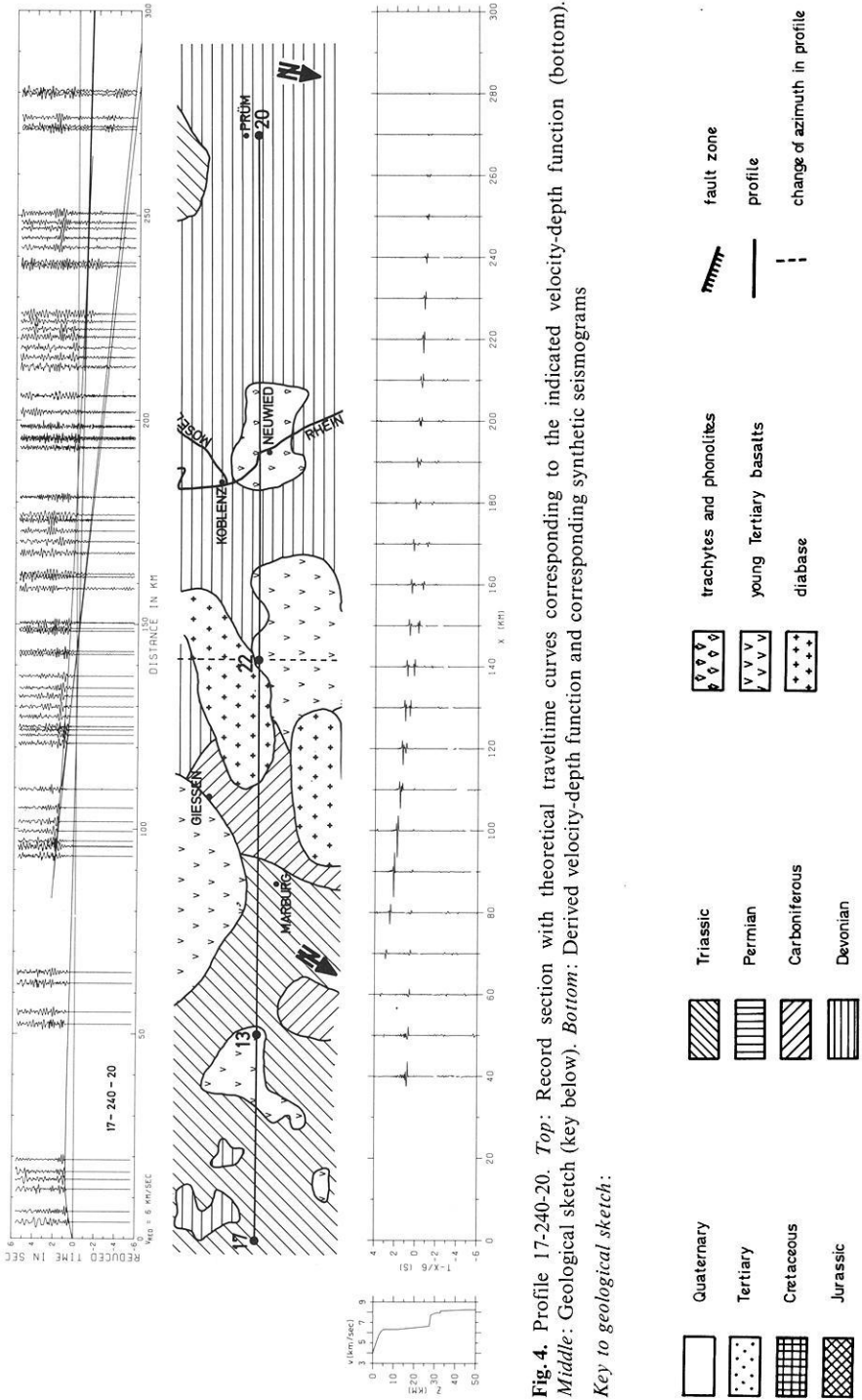
The general patterns of arrivals in the area of investigation can be divided into three types (Figure 3). In type I, we correlate only the  $P_g$ ,  $P_mP$  and  $P_n$  arrivals. In type II, in addition to these phases we correlate, beginning at a distance range of 60–90 km, a reflected phase between  $P_g$  and  $P_mP$ , named here  $P_iP$ . Type III, similar to type I, shows only one reflected phase. However, its apparent velocity at the critical distance is much lower than that of the  $P_mP$  phase in type I. For this reason we here refer to it as  $P_iP$ . The identification of these three types of the pattern of arrivals is important because each type corresponds to a distinct kind of crustal structure. It should be pointed out, however, that the phases  $P_mP$  and  $P_iP$  are not always true reflections, but often diving waves in a strong gradient zone on top of the corresponding boundary.

#### Type I: Data and Interpretation

Figures 4–8 show record sections representing type I. The first four profiles (17-240-20, 13-240-20, 22-060-13 and 20-070-22) constitute a reversing and over-



**Fig. 3.** Three types (I, II, and III) of basic traveltime diagrams identified in the area of investigation (see text for explanation of phases). Each type corresponds to a distinct kind of crustal velocity-depth structure



**Fig. 4.** Profile 17-240-20. *Top:* Record section with theoretical traveltimes curves corresponding to the indicated velocity-depth function (bottom). *Middle:* Geological sketch (key below). *Bottom:* Derived velocity-depth function and corresponding synthetic seismograms

*Key to geological sketch:*



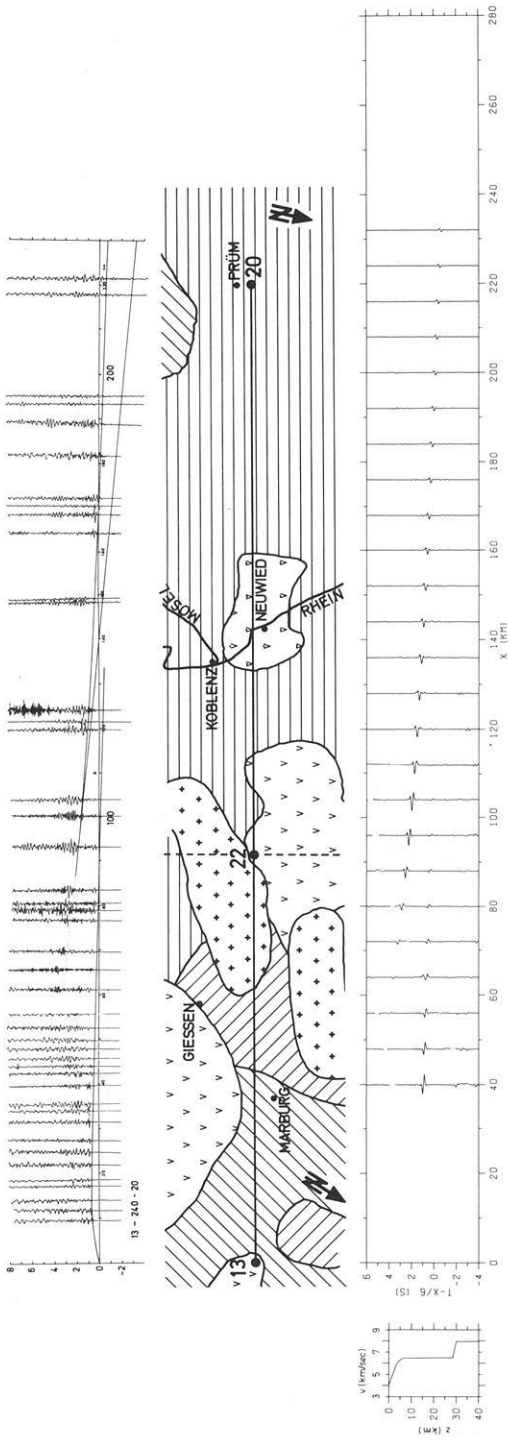


Fig. 5. Profile 13-240-20. *Top*: Record section and theoretical traveltime curves for indicated velocity-depth function. *Middle*: Geological sketch (key given in Fig. 4). *Bottom*: Velocity-depth function and corresponding synthetic seismograms

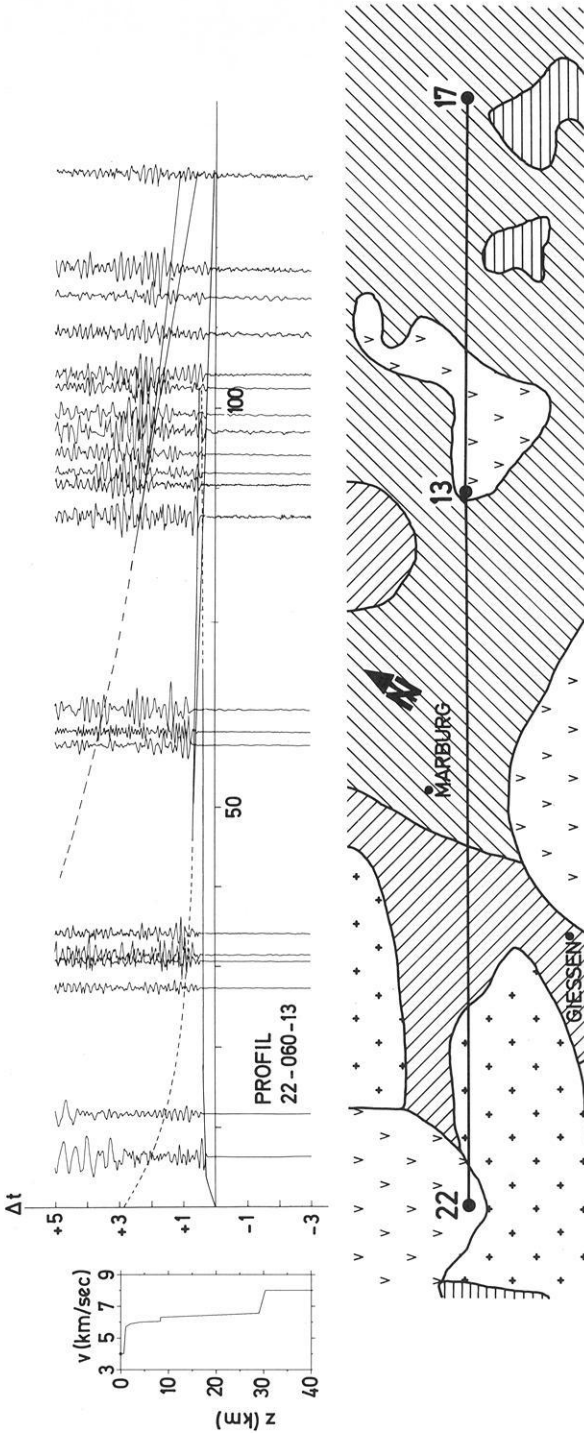


Fig. 6. Profile 22-060-13. *Top*: Record section with theoretical traveltime curves for indicated velocity-depth function. Broken lines: sub-critical reflections. *Bottom*: Geological sketch (key given in Fig. 4)

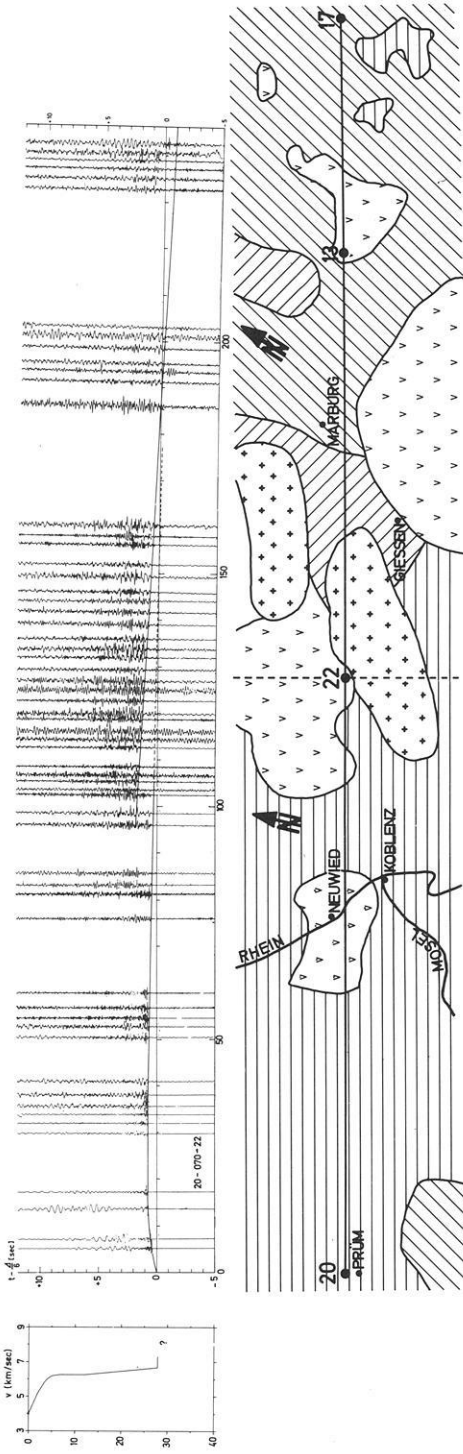


Fig. 7. Profile 20-070-22. *Top*: Record section and theoretical traveltime curves for the indicated velocity-depth function.  $P_n$  arrivals are not present. *Bottom*: Geological sketch (key given in Fig. 4)

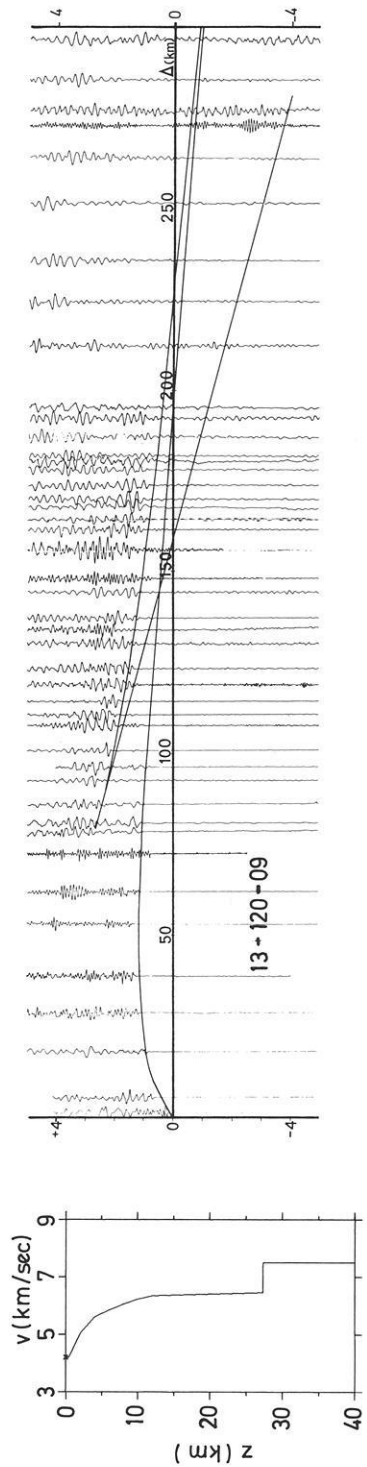


Fig. 8. Profile 13-120-09. Record section and theoretical traveltime curves for the indicated velocity-depth function

**Table 2.** Velocity-depth models shown in Figure 21. The number of each model refers to the profile shown in Figure 1 from which it is derived

Depth (km)	Velocity (km/s)	Depth (km)	Velocity (km/s)	Depth (km)	Velocity (km/s)	Depth (km)	Velocity (km/s)
02-165-01		02-215		02-220-05		02-265	
0.0	4.0	0.0	4.5	0.0	3.5	0.0	3.5
0.6	4.0	2.0	5.45	0.5	3.5	0.5	3.5
1.3	5.7	4.0	6.0	2.0	5.8	2.0	5.7
4.0	6.0	6.0	6.15	4.0	5.95	3.0	5.8
8.5	6.1	12.0	6.25	8.0	6.28	8.0	6.0
24.0	6.4	13.5	6.25	13.5	6.28	19.8	6.0
27.0	6.8	13.5	5.8	13.5	5.9	19.8	6.5
27.0	7.3	19.7	5.8	20.0	5.9	27.8	7.05
31.0	8.0	19.7	6.75	21.0	6.6	29.8	8.1
34.0	8.0	27.5	6.8	22.0	6.7		
34.0	8.1	28.5	8.3	22.0	6.0		
		33.0	8.48	26.5	6.0		
				26.5	7.0		
				27.5	8.2		
02-350-06		03-250		06-170-02		06-260	
0.0	4.2	0.0	3.1	0.0	4.0	0.0	4.0
0.8	4.2	0.5	3.1	1.3	4.0	1.6	4.0
2.0	5.65	2.0	6.06	3.0	5.6	2.0	5.0
4.0	6.0	4.0	6.15	6.0	6.0	3.3	5.8
6.0	6.2	5.0	6.15	22.2	6.4	6.3	6.0
8.0	6.31	14.8	6.2	22.2	6.8	10.0	6.05
10.0	6.35	14.8	5.5	31.5	8.0	10.0	6.0
28.8	6.35	23.3	5.5			14.0	6.0
30.5	7.9	23.3	7.25			14.0	6.3
		28.0	8.0			27.5	6.6
						28.8	8.0
08-000		12-260		13-120-09		13-240-20	
0.0	4.35	0.0	3.5	0.0	4.2	0.0	4.0
1.8	4.35	2.0	5.5	0.4	4.2	3.4	5.9
2.5	5.35	4.0	5.9	2.0	5.05	4.5	6.2
4.7	6.11	6.0	6.1	4.0	5.6	6.5	6.4
8.0	6.11	8.0	6.2	6.0	5.85	12.0	6.4
8.0	6.0	12.0	6.2	8.0	6.05	28.1	6.5
14.0	6.0	12.0	5.8	10.0	6.2	29.6	7.8
14.0	6.3	18.0	5.8	12.0	6.35		
26.2	6.4	18.0	6.4	27.3	6.45		
27.5	7.9	20.0	6.45	27.3	7.5		
		20.0	5.85				
		24.0	5.85				
		24.0	7.4				
		27.0	8.05				

Table 2 (continued)

Depth (km)	Velocity (km/s)	Depth (km)	Velocity (km/s)	Depth (km)	Velocity (km/s)	Depth (km)	Velocity (km/s)
14-010		14-090-02		16-080		17-240-20	
0.0	4.2	0.0	3.0	0.0	3.0	0.0	4.0
1.0	4.6	0.3	3.0	0.5	3.0	3.0	5.75
4.0	5.8	1.0	5.0	1.5	5.0	4.0	6.1
6.0	5.95	4.0	5.85	4.0	6.1	5.2	6.3
8.0	6.1	6.0	6.0	6.0	6.2	12.0	6.3
12.0	6.15	8.1	6.1	8.0	6.25	27.5	6.6
21.4	6.15	12.0	6.25	28.5	6.6	28.2	7.7
21.4	6.9	12.0	5.8	31.0	8.4	31.0	7.9
(27.0	8.0)	20.0	5.8			33.0	8.08
		20.0	6.6			45.0	8.17
		26.0	6.8				
		32.0	8.1				
20-070-22		22-060-17		240-LO-060			
0.0	4.0	0.0	4.0	0.0	5.25		
3.4	5.8	0.6	4.0	0.3	5.5		
4.0	6.0	1.0	5.7	0.6	5.9		
6.7	6.25	2.0	5.7	2.1	6.35		
12.0	6.25	2.0	5.9	6.0	6.35		
27.8	6.65	4.0	6.0	6.0	6.15		
27.8	7.3	8.3	6.05	15.8	6.15		
(32.0	8.0)	8.3	6.3	15.8	6.65		
		29.0	6.55	17.0	6.65		
		30.3	8.0	17.0	6.45		
				22.2	6.45		
				22.2	6.70		
				23.7	6.70		
				23.7	6.45		
				29.0	6.45		
				30.0	8.1		

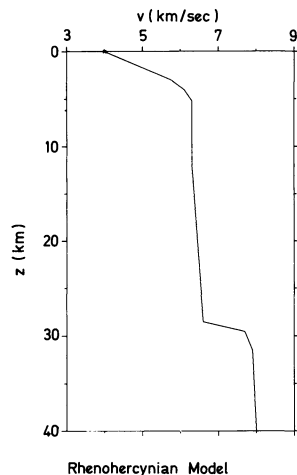
lapping system from the Hessische Senke into the Eifel (Figs. 1 and 2). As can be seen on the geologic sketches of Figures 4, 5 and 7, the line avoids significant contact with the young Tertiary basalts of the Vogelsberg and the central Westerwald, but passes through the trachytes and phonolites of the eastern Eifel and adjacent Neuwieder Becken. The fifth profile of type I discussed here, 13-120-09, is located completely outside of the Rhenish Massif.

On all profiles the phases  $P_g$  and  $P_mP$  are clearly visible,  $P_mP$  being always the dominant secondary arrival at distances greater than 90 km.  $P_n$  is visible to a varying degree on all profiles of sufficient length (i.e. more than 200 km) except on profile 20-070-22. A slight deviation from the type I-pattern of arrivals is exhibited in profile 22-060-13. Here an additional phase has to be correlated following the  $P_g$  phase by about 0.25 seconds.

For all profiles individual velocity-depth functions have been determined (Figs. 4–8). The corresponding computer-produced traveltimes curves have been superimposed on the data. Table 2 lists all velocity-depth functions discussed in this paper. In addition, for profiles 17-240-20 and 13-240-20 synthetic seismograms are shown in Figures 4 and 5. On profiles 17-240-20, 13-240-20 and 20-070-13 the crustal structure is very similar. The velocity increases continuously with depth reaching 6.3 km/s at about 5 km. With further depth it increases only a few tenths of km/s before reaching the crust-mantle boundary. For profiles 22-060-13 and 13-120-09 the velocity-depth functions look similar except for the upper crust.

The structure of the crust-mantle boundary is variable. On profiles 17-240-20, 13-240-20 and 22-060-13 it consists of a thin transition zone at 28–30 km depth with a strong velocity increase from 6.6 to 7.8–8.0 km/s. Profiles 20-070-22 and 13-120-09 show a strong velocity increase up to only 7.3–7.5 km/s; for the former, detailed knowledge of upper-mantle structure is lacking due to the absence of  $P_n$  arrivals; for the latter,  $P_n$  arrivals indicate that a low velocity of  $\sim 7.5$  km/s seems to continue to greater depths beneath the Moho. For profile 17-240-20 a greater resolution of the structure immediately beneath the Moho can be obtained. Strong  $P_n$  arrivals and especially the  $P_n/P_mP$  amplitude relationship suggests positive velocity gradients and a velocity step in the uppermost mantle as shown in Figure 4 (see also Table 2).

From the preceding five profiles the following conclusion seems to be justified: the data obtained in the area between shotpoints 20 and 17 define a similar and relatively simple crustal model. In concordance with the geologic province, this model is here referred to as the Rhenohercynian Model (Fig. 9). Basically it is characterized by a rather homogeneous crust between 5 and 28 km depth where the velocity increases only slightly from 6.3 to 6.6 km/s, a thin crust-mantle transition of about one kilometer thickness within which the velocity increases rapidly up to about 7.7 km/s and an additional positive velocity



**Fig. 9.** Rhenohercynian model. Standard crustal model based on the common results of several seismic profiles (see discussion in the text)

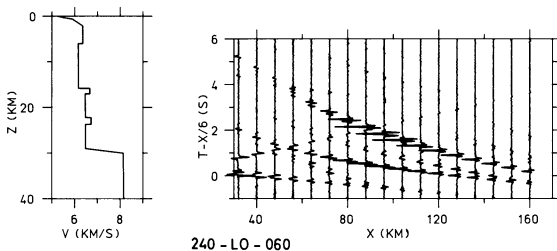
gradient beneath the Moho which produces an average upper-mantle velocity of 7.9–8.0 km/s.

### *Type II: Data and Interpretation*

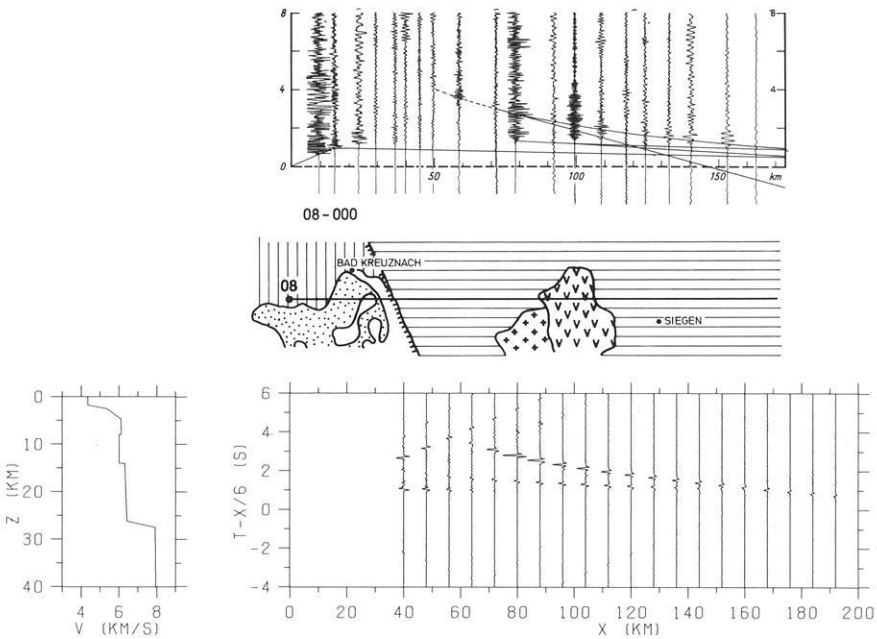
The profiles of type II show greater variability in crustal structure than those of type I. As mentioned above, in addition to the  $P_mP$  phase, a second phase, named here  $P_iP$ , can be correlated in later arrivals. This phase may be either weaker or stronger than the  $P_mP$  phase. The profiles where  $P_mP$  is dominant will be discussed first.

The original data of profile 240-LO-060 (Fig. 10), a specially planned wide-angle reflection profile with a common depth point along the strike of Hunsrück and Taunus, are published by Giese et al. (1976, Appendix, Map 3, record section 62) and Meissner et al. (1976a, Fig. 3). Profiles 08-000 (Fig. 11) and 06-260 (Fig. 12) are observed from shotpoints outside the Rhenish Massif. 08-000 crosses the Saar-Nahe-Trough, Taunus and Westerwald in south-north direction, while 06-260 is located at the northern margin of the Rhenish Massif extending westward from the Solling into the Ruhrgebiet. All three profiles show a strong  $P_mP$  phase as the dominant feature in the secondary arrivals; however, an additional phase can be correlated indicating an intermediate crustal reflector at about 15 km depth, where the velocity increases from about 6.0 to 6.4 km/s. Similar to the profiles of type I, the presence of clear  $P_mP$  arrivals at approximately 80–100 km distance defines a relatively thin crust-mantle transition zone,  $\sim 1$  km thick, with a strong velocity increase. The velocity structure beneath the Moho is rather uncertain because these profiles extend to a maximum range of only 160 to 190 km and show only very weak indications of  $P_n$ .

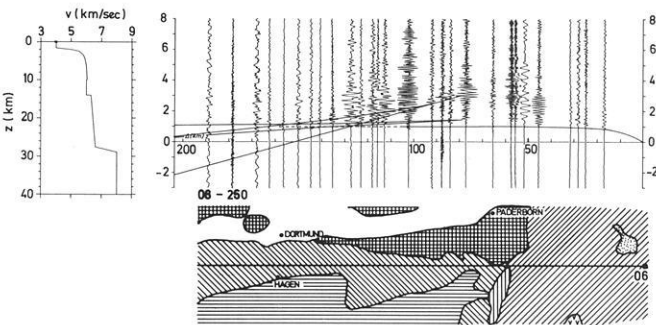
The profiles 14-090-02 and 02-265 (Fig. 13) can also be regarded as belonging to type II. Both profiles cross the young Tertiary volcanics of the Vogelsberg and the central Westerwald. In contrast to the profiles just discussed, the  $P_mP$  phase is not the dominant secondary arrival. Rather, the strongest arrivals are formed by a phase reflected from a boundary within the lower crust at about 20 km depth. For these profiles a 6–8 km thick crust-mantle transition is derived by traveltimes and amplitude modelling. Also the observed  $P_n$  velocity ( $\sim 8.1$  km/s) is greater than on the adjacent profiles.



**Fig. 10.** Profile 240-LO-060. Derived velocity-depth function and synthetic seismograms



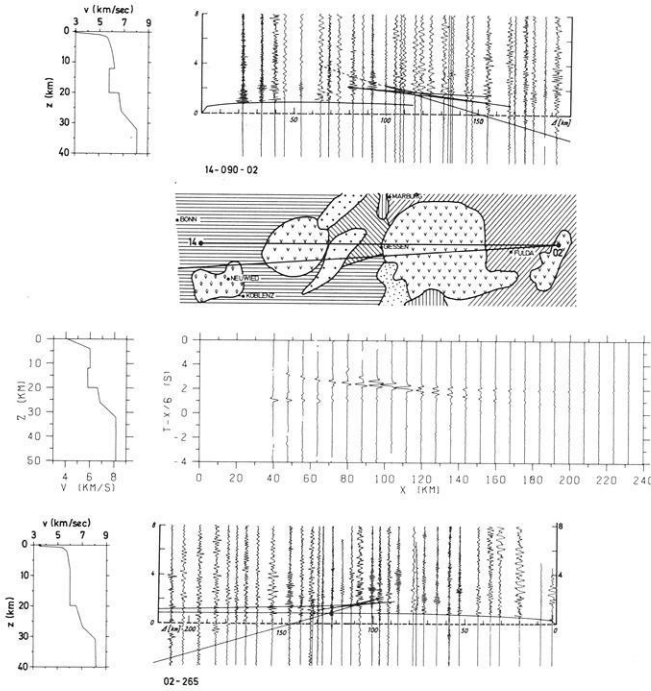
**Fig. 11.** Profile 08-000. *Top*: Record section with theoretical traveltime curves for the indicated velocity-depth function (bottom left). Broken line: sub-critical reflection. *Middle*: Geological sketch (key given in Fig. 4). *Bottom*: Derived velocity-depth function and synthetic seismograms



**Fig. 12.** Profile 06-260. *Top*: Record section with theoretical traveltime curves for the indicated velocity-depth function. *Bottom*: Geological sketch (key given in Fig. 4)

In profile 14-090-02 the close fitting of the traveltimes of the  $P_g$  phase (upper part of Figure 13) produces high amplitude  $P_g$  arrivals which do not agree with the observed  $P_g/P_iP$  amplitude ratio. Consequently in the synthetic-seismogram calculations the upper crust has been simplified to produce amplitude ratios closer to those observed (middle part of Fig. 13). The resulting traveltime deviations are less than 0.2 seconds and may be attributed to lateral inhomogeneities.



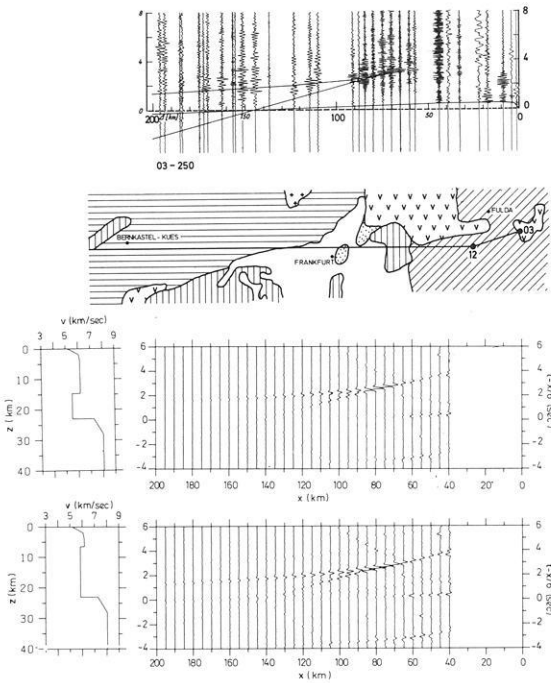


**Fig. 13.** Profiles 14-090-02 and 02-265. *Top:* Record section for profile 14-090-02 with theoretical traveltim curves for the given velocity-depth function. Broken line: sub-critical reflections. Geological sketch shows the locations of the shotpoints 14 and 20 (key given in Fig. 4). *Middle:* Velocity depth functions and corresponding synthetic seismograms. The best match to the data of profile 14-090-02 is obtained with a zero velocity gradient in the upper crust. *Bottom:* Record section for profile 02-265 with theoretical traveltim curves for the given velocity-depth function

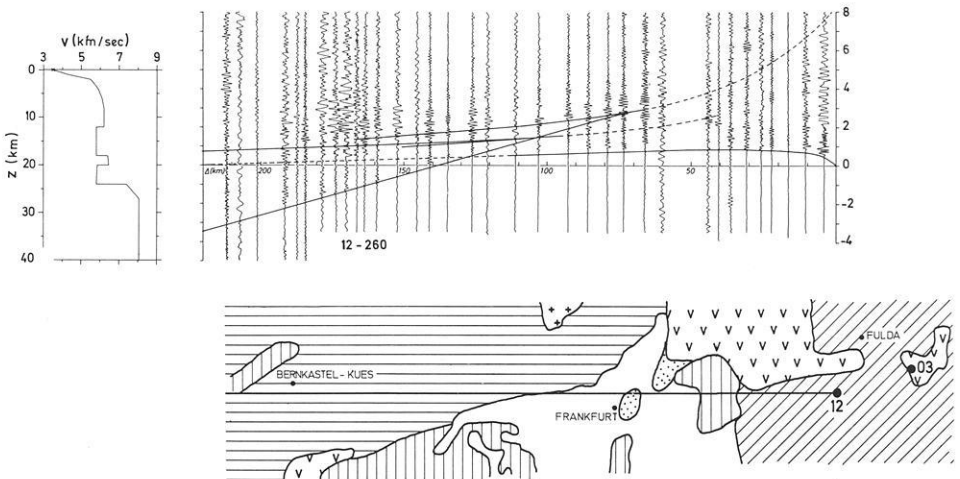
A feature general to all profiles of type II is a lower average velocity ( $\sim 6.0$  km/s) in the depth range between 5 and 15–20 km than that observed on most profiles of type I ( $\sim 6.3$  km/s).

*Type III: Data and Interpretation*

Two of the profiles discussed here, 03-250 and 12-260, cross several geological units, and therefore lateral heterogeneities have to be suspected. Both profiles extend from the Hessische Senke through the northern end of the Rhine Graben into the Rhenish Massif. For profile 03-250 (Fig. 14) the later arrivals recorded up to 90 km distance are interpreted as a reflection, here called  $P_iP$ , from a boundary within one geological unit, the Hessische Senke. The velocity-depth structure based mainly on these and  $P_n$  arrivals is shown in Figure 14. The synthetic seismograms emphasize the indeterminate configuration of the crustal velocity inversion; both adequately model the large-amplitude ( $P_iP$ ) reflection arrivals which are observed between 65 and 90 km distance. The presence of



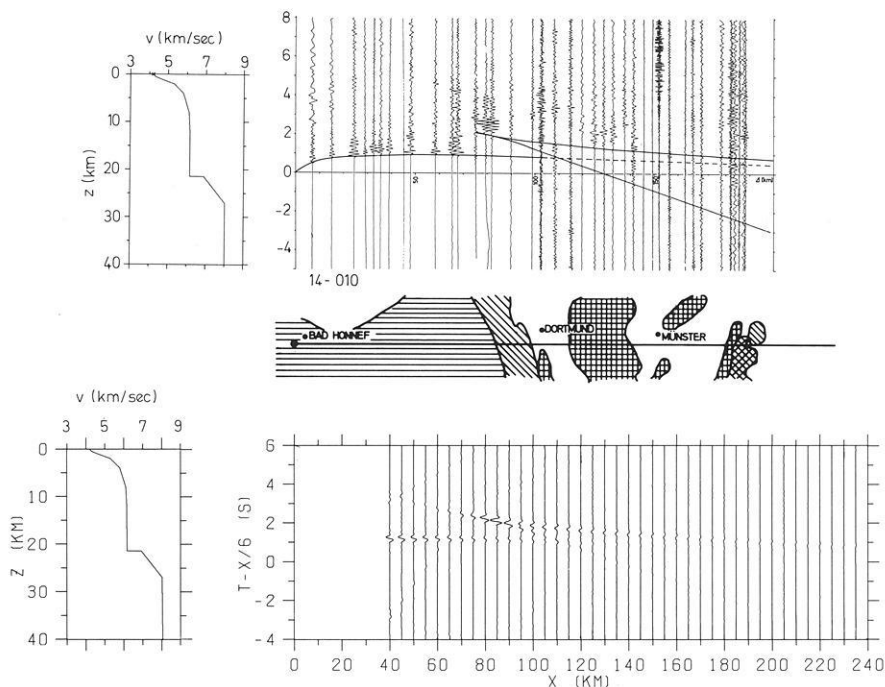
**Fig. 14.** Profile 03-250. *Top*: Record section with theoretical traveltime curves corresponding to the velocity-depth function given with the first synthetic seismograms. *Middle*: Geologic sketch (key given in Fig. 4). *Bottom*: Velocity-depth functions and synthetic seismograms. The area within the low-velocity zone is the same in the two velocity-depth functions. Both synthetic seismograms are in good agreement with the observed data



**Fig. 15.** Profile 12-260. *Top*: Record section and theoretical traveltime curves for the indicated velocity-depth function. Broken lines: subcritical reflections. *Bottom*: Geologic sketch (key given in Fig. 4)

this phase can also be recognized, although less clearly, in profile 12-260 (Fig. 15). For both profiles, the low apparent velocity of the  $P_1P$  phase and the well-defined  $P_n$  phase are best modelled as shown in Figures 14 and 15. At a depth of 23–24 km the velocity increases rapidly from less than 6 to about 7.3 km/s. The velocity increases then gradually with depth, reaching an upper-mantle velocity of 8.0 km/s at 27–28 km depth. In profile 12-260 we have indicated an additional phase between  $P_g$  and  $P_1P$  indicative of a complex structure within the region of general velocity decrease. Scattered arrivals between  $P_g$  and  $P_1P$  are also present in profile 03-250, but have not been modeled.

A similar  $P_1P$  phase is observed on profile 14-010 (Fig. 16) extending northward from the Siebengebirge through the Rhenish Massif into the Münsterländer Bucht. At about 100 km distance a phase is weakly indicated in later arrivals which if interpreted as a remnant of a reflected phase would yield a depth of about 30 km. However, because of its uncertainty it is not taken into account for the calculation of the velocity-depth function. The  $P_n$  phase is poorly recorded due to the sediments in the Münsterländer Bucht. The derived velocity-depth function shown with synthetic seismograms in Figure 16 is similar to those of profiles 03-250 and 12-260, but does not show a velocity inversion within the crust.



**Fig. 16.** Profile 14-010. *Top:* Record section and theoretical traveltimes for the indicated velocity-depth function. *Middle:* Geologic sketch (key given in Fig. 4). *Bottom:* Derived velocity-depth function and synthetic seismograms

### Crustal Structure of the Rhenish Massif

In Figures 17 and 18 an attempt has been made to compile the main features of crustal structure along two selected lines through the Rhenish Massif. The first line (Fig. 17) crosses the Rhenish Massif in an E-W direction (AA' in Fig. 2). The eastern part of the cross section is located in the Hessische Senke, showing a structure which looks very similar to the Rhenohercynian type: a rather homogeneous crust separated from the upper mantle by a well-defined crust-mantle transition zone. Continuing to the west, beneath the Vogelsberg, the crustal structure gets more complicated. The main features are a seismic discontinuity at a depth of 20 km and the replacement of a clear crust-mantle boundary by a wide transition zone. Entering the Rhenish Massif the Rhenohercynian structure is again encountered. The area of the central Westerwald, covered by young Tertiary basalts, however, shows an anomalous structure similar to the one evident beneath the Vogelsberg. In contrast, the area covered by trachytes and phonolites further to the west in the eastern Eifel and adjacent Neuwieder Becken, while apparently showing an undisturbed Rhenohercynian

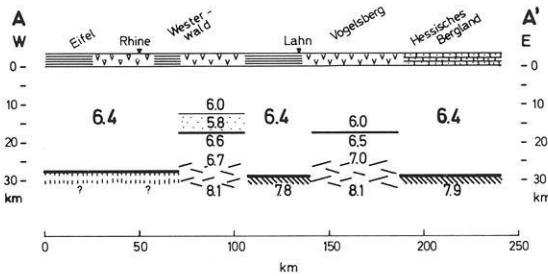


Fig. 17. Cross section through the Rhenohercynian zone (AA' in Fig. 2).

*Explanation:* Tertiary and Quaternary sediments, Triassic, Devonian, Young Tertiary basalts, Trachyte and Phonolite, strongly reflecting boundary, boundary causing weak or scattered reflected phases, interpolated boundary, positive velocity gradient within the lower crust, upper mantle producing clear P<sub>n</sub> arrivals, upper mantle producing weak or no P<sub>n</sub> arrivals, crustal velocity inversion, **6.1** average crustal velocity below 3 km depth, **6.1** velocity above or below a boundary

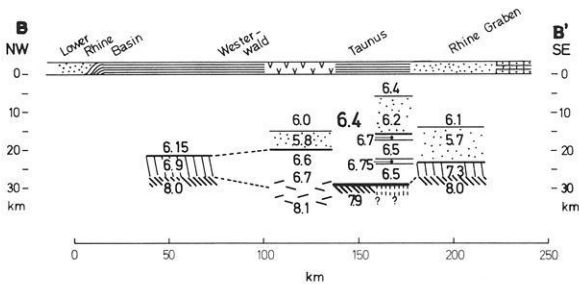
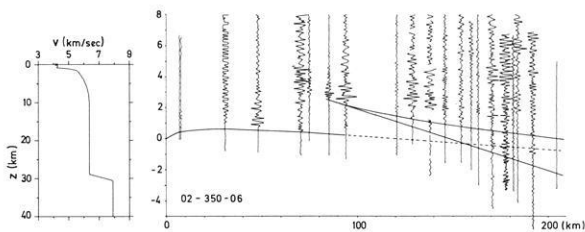


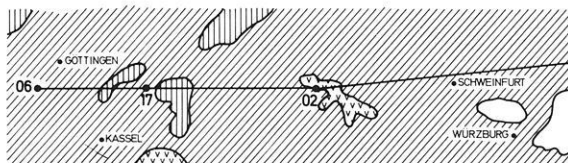
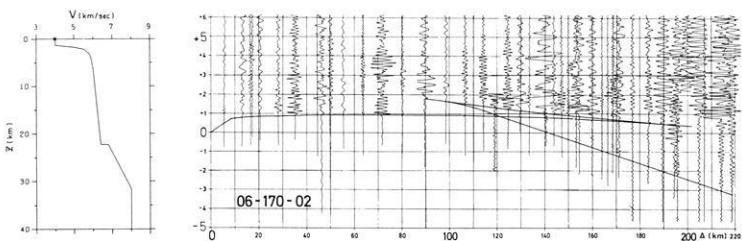
Fig. 18. Cross section through the Rhenohercynian zone (BB' in Fig. 2). Explanation see Fig. 17

crustal structure, shows an anomalous mantle: the clear  $P_mP$  arrivals reach an apparent velocity of only 7.3 km/s, and  $P_n$  arrivals are not at all visible.

The second line (Fig. 18) crosses the Rhenish Massif in a NW-SE direction (BB' in Fig. 2). The northern part of the section is located at the edge of the Lower Rhine basin. Although it is not evident from its geologic setting, the Rhenish Massif in the region east of Cologne shows an unexpectedly anomalous crustal structure: a seismic discontinuity is apparent at about a 21-kilometer depth followed by an apparently smooth and continuous transition to the upper mantle. Towards the southeast, east of the Siebengebirge, no data are available. The volcanic area of the central Westerwald, whose crustal structure also appears in section AA', also exhibits an intermediate crustal boundary and wide crust-mantle transition zone. Comparing this structure with that observed east of Cologne, it can be suggested that the Rhenish Massif east of the Siebengebirge also consists of a similar anomalous crust. South of this volcanic area the Rhenohercynian crust is encountered. Upon entering the Taunus, the densely-recorded profile (240-LO-060) has revealed a more complex crustal structure whose main features are pronounced discontinuities at about 16 km and 29 km depths. Due



**Fig. 19.** Profile 02-350-06. Record section and theoretical traveltime curves for the indicated velocity-depth function. Broken line: weak  $P_g$  arrivals. The geologic location of the profile is given in Fig. 20



**Fig. 20.** Profile 06-170-02. *Top*: Record section and theoretical traveltime curves for the indicated velocity-depth function. *Bottom*: Geologic location of profiles 02-350-06 and 06-170-02 (key given in Fig. 4). Strong lateral heterogeneity of crustal structure is evidenced by the differing velocity-depth functions obtained for these reversing profiles (see text)

to the manner of recording and incomplete length of the profile 240-LO-060 it cannot be conclusively stated whether the lack of  $P_n$  arrivals is due to mantle velocity structure. Entering the northern end of the Rhinegraben the crustal structure changes yet again: a low-velocity upper crust reaching a discontinuity at 23–24 km is followed by a high-velocity lower crust which gradually reaches upper mantle velocity.

Similar to the two cross-sections just discussed, a rapid change in crustal structure is evident along the line between shotpoints 02 and 06 in the Hessische Senke. The observed data of profiles 02-350-06 and 06-170-02 shown in Figures 19 and 20 evidently do not contain phases representing reflections from the same depth range. The independently derived velocity-depth functions shown with the data are of type I and III, respectively, though they represent crustal structures separated by only 25 km distance. Thus, though it is not evident from the geologic setting, strong lateral heterogeneities are indicated for this region.

## Discussion

The results are summarized in Figures 21 and 22. Figure 21 shows the geographic location of the velocity-depth functions obtained for each individual profile, each inlet being placed approximately in the area for which it is representative. Figure 22 summarizes the main features of crustal structure. To a certain extent these maps reflect the features discussed for the individual profiles as type I, II and III. For the major part of the area of investigation a strong reflection from a depth of 28–30 km is found. For the areas of young Tertiary volcanism, this reflection is only weakly indicated, and in three widely separated areas none is observed.

A similar variation is observed for intracrustal reflectors, which some authors refer to as Conrad or/and Sub-Conrad boundaries (e.g. Meissner et al., 1976a).

Such a reflector is notably absent in a large area north and east of the Vogelsberg and in the Eifel west of the Rhine. In contrast, the Hunsrück and Taunus as well as some areas at the northeastern and southeastern edge of the Rhenish Massif do contain intracrustal reflectors. In the areas of young Tertiary volcanism this intracrustal reflector produces by far the dominant phase. Finally, there do exist areas where only a strong reflection from depths within the crust is obtained, while the crust-mantle boundary is only indicated by a gradual transition from crustal to upper-mantle velocities.

The results obtained by the reinterpretation of the profiles discussed in the previous sections differ in detail but in general strengthen and confirm the results published by various authors at earlier stages. Fritsch (1971) discusses in detail results of short-range refraction measurements in the Siegerland. His results for the uppermost crust are confirmed by those presented here for profiles 14-010 and 14-090-02 which cross the neighbouring regions. In the same geographic area, Dürbaum et al. (1971) report the recording of strong reflections with 5–7 seconds two-way traveltime. This may correspond to the strong reflector at about 20 km depth found on both profiles radiating from shotpoint 14 (see Fig. 21), thus supporting the assumption that such a boundary may continue

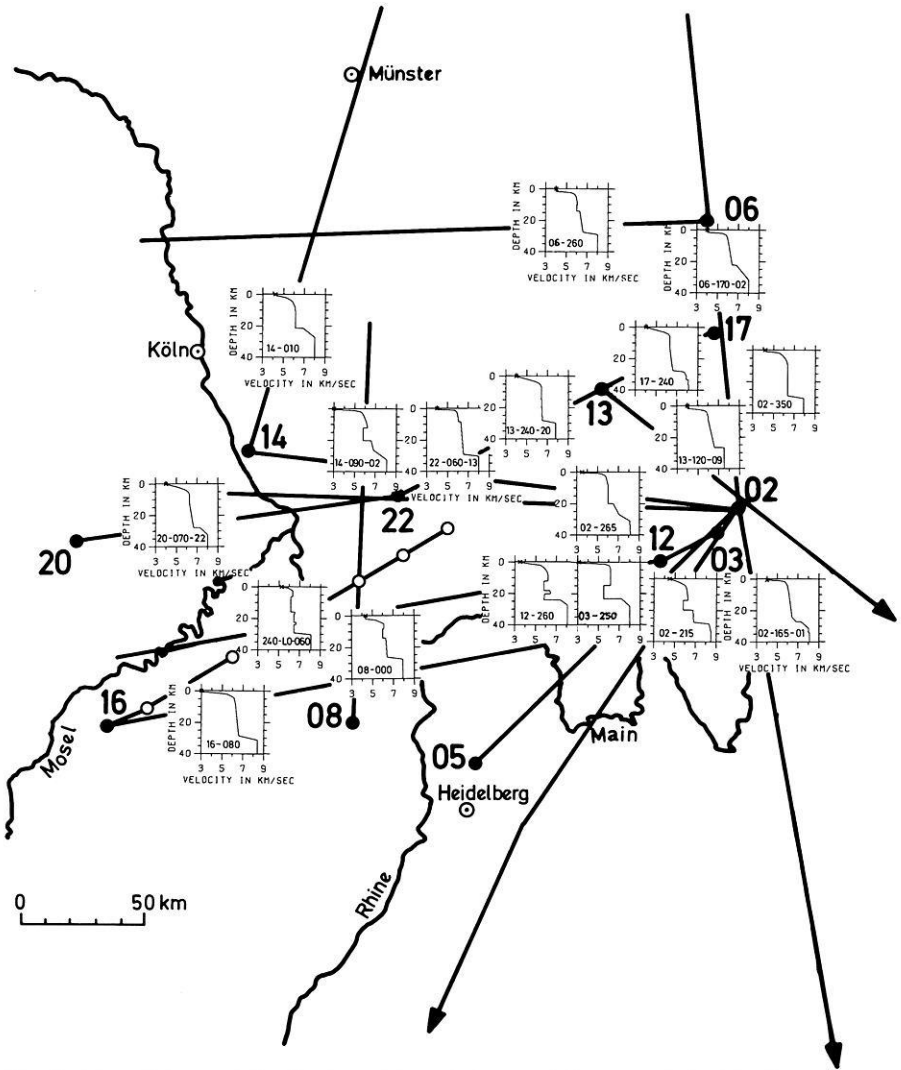


Fig. 21. Map of the areal distribution of the velocity-depth functions derived in the present study. The shot-points are indicated in bold letters. The velocity-depth functions are representative for the area into which they have been placed (see text for discussion)

from the central Westerwald towards the north and northwest, as indicated in Figure 18.

The interpretation of the profile 240-LO-060 is based on our agreement with the phase correlation published by Meissner et al. (1976a). It is therefore not surprising that despite some minor differences the results of depth determination correspond quite well. The major difference is that our M-discontinuity is sharper than that proposed by Meissner et al. (1976a). Though the data of the profile 08-000 are not of good quality, the agreement of the resulting model with the model obtained for profile 240-LO-060 is surprisingly good! As shown by Glocke and Meissner (1976), the interpretation of these

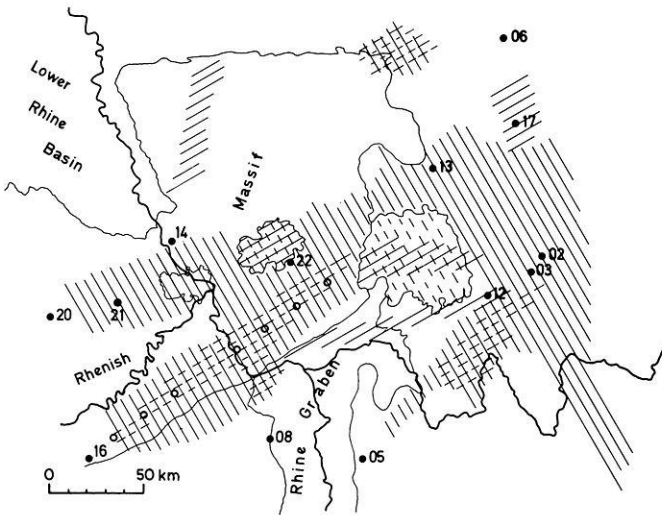

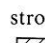
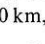
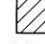


Fig. 22. Map of the area of the Rhenohercynian zone showing main features of crustal structure. Explanation:  strong reflection from a depth of 28-30 km,  weak reflection from a depth of 28-30 km,  strong reflection from a depth between 10 and 22 km,  weak reflection from a depth between 10 and 22 km, ● shotpoints at quarries, ○ shotpoints of wide-angle profile. Profile lines are indicated in Figure 1

wide-angle measurements is in good agreement with that of the near-angle reflection survey carried out along the same line. The first results obtained by Bartelsen et al. (1975) for the seismic-reflection measurements along the geotraverse Rhenohertzynikum, which at its northern end crosses the line 240-LO-060, also indicate a similar depth range of the main reflectors.

Profile 20-070-17 has been interpreted by Weber (1973). The corresponding velocity-depth function given here shows the same average properties of upper and lower crust, but differs in the shape of the crust-mantle boundary. As  $P_n$  arrivals have not been recorded on this profile it can neither be decided whether the velocity reaches values of 8 km/s nor to which depth the crust-mantle transition zone extends. The lack of  $P_n$  on this profile does, however, argue against strong positive velocity gradients below the crust-mantle discontinuity.

The particular shape of the velocity-depth distribution for the area of the northern end of the Rhine Graben has been discussed by Meissner et al. (1976 b), who also obtain a gradual transition below a reflector at about 22 km depth, below which the velocity increases gradually towards upper-mantle values without forming a distinct crust-mantle boundary. A similar shape of the crust-mantle transition zone is also found for the southern Rhine Graben proper (Edel, 1975; Edel et al., 1975; Prodehl et al., 1976).

The line between shotpoints 02 and 06 and its northward and southward extension has been previously intensively studied (see, e.g., Fuchs and Landisman, 1966 a, b; Wangemann, 1970). Corresponding to the result shown in Figure 20 for profile 06-170-02, Fuchs and Landisman (1966 b) describe a 7.2 km/s refraction line which is also evident in the crustal model which the authors



regard as representative for the South German Triangle. However, in comparing profiles 02-350-06 and 06-170-02, they do not make note of the strong lateral changes which are commented on in the present paper.

The most extensive discussion of the data reinterpreted in this paper has been published by Giese and Stein (1971) and Giese (1976a). These papers summarize all quarry blast data available in Western Germany, and Giese (1976b) discusses them within the corresponding geological framework. Similar to the results shown in Figures 21 and 22, Giese (1976a) shows areas of reduced upper-mantle velocities which, according to his interpretation, are connected with decreased crustal thickness. In our interpretation, we have defined a reflector at about 22 km depth as an intracrustal reflector beneath which the velocity increases gradually to upper-mantle velocity values. Giese's (1976b) conclusion that the existence of a wide crust-mantle transition is connected with areas where young Tertiary volcanism occurred is confirmed by our reinterpretation.

### Conclusions

Although there are some gaps in the data in the profiles between shotpoints 17 and 20, it can be stated that the absence of an intermediate phase  $P_iP$  is due to crustal structure and not due to insufficient data. The  $P_n$  phases also show varying quality, being well recorded on the profile 17-240-20 and apparently absent on profile 20-070-17. This lateral variability may correspond to that which is well known from the results of reflection profiles.

According to the geological situation the Devonian and lower Carboniferous sediments of the Rhenish Massif continue into the Hessische Senke beneath a thin cover of Buntsandstein and Tertiary sediments which at the most are only some hundred meters thick (Henningsen, 1976). This is in agreement with the result described in this paper that in general a "Renohercynian model" can be derived both for the Rhenish Massif and the Hessische Senke, as far as they are not covered by extensive volcanic features. In this context it is to be questioned why the Hessische Senke did not take part in the uplifting process of the Rhenish Massif.

As has been also observed by Giese (1976b), the influence of volcanic events on crustal structure is significant. This is shown in the cross section traversing the Rhenish Massif in an E-W direction (Figure 17). The crustal structure beneath the volcanic area of the eastern Eifel and adjacent Neuwieder Becken (which is covered mainly by phonolites and trachytes) is very different from the structure beneath the central Westerwald and the Vogelsberg where young Tertiary basalts are exposed. The petrologic differences seem to explain the differing seismic wave propagation. The tholeiitic magmas of the Vogelsberg and the central Westerwald may originate within the upper mantle at depths greater than 60 km. During their eruption through the crust the crust-mantle boundary has been heavily disrupted and to a certain extent been replaced by a boundary at intermediate depths of about 20 km. The alcaic volcanism of the eastern Eifel has evidently influenced the upper mantle immediately beneath the Moho, and so attenuates the propagation of  $P_n$  waves penetrating

into the uppermost parts of the mantle. There remains, however, a sharp crust-mantle boundary thus giving the strong reflection of seismic energy.

The continuation with depth of surficially visible volcanic and tectonic features is also reflected in the nature of the crustal structure and the crust-mantle transition in other areas. For example, the crustal structure of the central Massif of France changes rapidly when crossing the Limagne Graben and the volcanic areas of the Auvergne as shown by Perrier and Ruegg (1973) and Hirn and Perrier (1974).

As is evident from the cross sections in Figures 17 and 18, and the maps in Figures 21 and 22, in areas where weak or no Moho reflection is found the intracrustal reflector at about a 20–22 km depth produces strong reflected seismic energy. For the southern Rhine Graben Edel et al. (1975) have shown a highly anomalous crust-mantle transition between 20 and 25 km, which may be caused by mass intrusion from the upper mantle or by phase transformations. A similar anomalous structure is also found in that part of the northern Rhine Graben covered by this investigation, and may also be valid for the area east of Cologne and the areas of young Tertiary volcanism. While the crustal structure typical for the Rhine Graben area definitely terminates at the northern end of the Vogelsberg it may be suggested that the Rhine Graben-like crustal structure is also present in the area east of Cologne and the Lower Rhine Basin. While no crustal information is available for the Lower Rhine Basin proper it has been observed (e.g., Ahorner, 1970; Bonjer, 1977) that an earthquake activity similar to that of the Rhine Graben area is observed in parts of the Rhenish Massif and the Lower Rhine Basin.

Concerning the Rhenish Massif proper, the map showing the main features of crustal structure (Figure 22) also indicates a division of the Rhenish Massif parallel to its strike. While the southern part—Hunsrück and Taunus—shows some structure within the crust, the central part—Westerwald and Eifel—is characterized by a more homogeneous crust. This is concordant with the geologic observation that the southern part of the Rhenish Massif has been subjected to a higher grade of metamorphism (Henningsen, 1976). Bonjer (1977) has shown that the areas showing a higher grade of metamorphism such as Hunsrück and Taunus in the south as well as Hohes Venn (northern Eifel) in the northwest are connected with increased microearthquake activity. Also in the northeastern corner of the Rhenish Massif, which is traversed by profile 06-260, slightly increased metamorphism is indicated in the Lippstädter Gewölbe (Hoyer et al., 1974). It does not seem unreasonable to suggest that the areas, where a higher grade of metamorphism and increased seismicity are indicated, have been uplifted versus the adjacent areas and that eventually the intermediate crustal layer found here may be identified with a fossil crust-mantle boundary of pre-Tertiary times.

There remain many open questions which cannot be solved with the data available. Only little can be stated about the Hercynian basement beneath the Devonian and Carboniferous sediments. A special structure of the crust and the upper mantle beneath the Tertiary volcanic areas is clearly indicated by the existing data. However, for a detailed resolution, more data are required. The same is true for the possible differences between the Rhenish Massif and

the Hessische Senke; the structure we have presented here is very similar in these areas. Considering these uncertainties, a contour map of the depth of the crust-mantle boundary has not been constructed.

As only few profiles extend into distances beyond 150 km, the determination of the upper-mantle velocity is rather uncertain. Thus, it is also an open question to what areal extent  $P_n$  waves are attenuated when passing the region of Quaternary volcanism of the eastern Eifel. Bamford (1973, 1976a,b) has concluded, on the basis of a larger data set than considered here, that there is significant anisotropy in the upper-mantle P-wave velocity in Germany. As Figure 1 shows, the profiles considered in the present paper are not favorably arranged to detect azimuthal variations in  $P_n$  velocity. On the process of preparing this paper the authors did, however, note the indication of another sort of anisotropy, namely anisotropy in the  $P_n/P_m$  amplitude ratio. A more complete study of this type of anisotropy seems to be warranted at this time.

The results of this investigation are regarded as the basis for future work in order to fill gaps where necessary and to plan carefully towards the detailed investigation of the crustal structure of selected areas and towards the extension of our knowledge into the lower lithosphere, aiming especially towards the problem of vertical movements in the area of the Rhenish Massif and adjacent areas.

*Acknowledgments.* The authors are indebted to K. Fuchs for his continuous support and special interest in this investigation. S. Faber, P. Giese, S. Hammer, W. Kaminski and G. Müller supported us with stimulating advice. Helpful discussions with J. Ansorge, D. Bamford, K. Bonjer, R. Emmermann, R. Meißner and A. Stein are gratefully acknowledged. R. Kind kindly provided his revised computer program of the reflectivity method. H. Bartelsen and R. Meissner, Kiel, M. Degutsch, Münster, W. Kaminski, Karlsruhe, A. Stein, Hannover, R. Veas, Clausthal, generously provided largescale record sections.

The research project was made possible by the support of the Deutsche Forschungsgemeinschaft. One of the authors (W.D.M.) was partially supported by NSF grant EAR76-14840 during his stay in Germany. Computation facilities were made available by the Geophysikalisches Institut and the computer center of Karlsruhe University.

## References

- Ahorner, L.: Seismo-tectonic relations between the graben zones of the Upper and Lower Rhine valley. In: Illies, H.; Mueller, S. (eds.): Graben problems, Stuttgart: Schweizerbart, 155-166, 1970
- Ansorge, J.; Emster, D.; Fuchs, K.; Lauer, J.P.; Mueller, S.; Peterschmitt, E.: Structure of the crust and upper mantle in the rift system around the Rhinegraben. In: Illies, H., Mueller S. (eds.): Graben problems, Stuttgart: Schweizerbart, 190-197, 1970
- Bamford, D.: Refraction data in western Germany—a timeterm interpretation. *Z. Geophys.* **39**, 907-927, 1973
- Bamford, D.: MOZAIC time-term analysis. *Geophys. J. Roy. Astron. Soc.* **44**, 433-446, 1976a
- Bamford, D.: An updated time-term interpretation of  $P_n$  data from quarry blasts and explosions in western Germany. In: Giese, P.; Prodehl, C.; Stein, A.: Explosion seismology in central Europe—data and results. Berlin-Heidelberg-New York: Springer 215-220, 1976b
- Bartelsen, H.: Deutung der seismischen Weitwinkelmessungen in der Rheinischen Masse unter Verwendung neuer Kontroll- und Auswerteverfahren. Diplomarbeit, Univ. Frankfurt, 90 p., 1970

- Bartelsen, H.; Meissner, R.; Murawski, H.: Seismic reflection measurements along the geotraverse Rhenoherynikum. Proc. 14th Ass. Europ. Seismol. Comm. (Trieste 1974), Berlin: Akad. Wiss. DDR, 245–251, 1975
- Behnke, C.: Bericht über die Auswertung refraktionsseismischer Messungen "Westprofil Thaiden". In: Niedersächsisches Landesamt für Bodenforschung (ed.): Kurzfassungen der Vorträge des DFG-Kolloquiums "Erforschung des tieferen Untergrundes in Mitteleuropa" in Frankfurt vom 4.–6.1.1961, NLFH Hannover, 7 p., 1961
- Bonjer, K.: Zusammenhänge zwischen Seismizität und lateralen Variationen der Krustenstruktur im Rheinischen Schild. In: Maronde, D. (ed.): Protokoll über das 2. DFG-Kolloquium im Schwerpunkt "Vertikalbewegungen und ihre Ursachen am Beispiel des Rheinischen Schildes" in Königstein vom 25.–26.11.1977, Deutsche Forschungsgemeinschaft Bonn, 76–79, 1977
- Closs, H.; Behnke, C.: Fortschritte der Anwendung seismischer Methoden in der Erforschung der Erdkruste, Geol. Rundschau **51**, 315–330, 1961
- Dürbaum, H.J.; Fritsch, J.; Nickel, H.: Reflexionsseismik. In: Lang, H.D. (ed.): Geologisch-lagerstättenkundliche und geophysikalische Untersuchungen im Siegerländer – Wieder Spateisenbezirk. Beih. geol. Jb. **90**, 99–124, 1971
- Edel, J.B.: Structure de la croûte terrestre sous le fossé Rhénan et ses bordures. Thèse, Univ. Strasbourg, 207 p., 1975
- Edel, J.B.; Fuchs, K.; Gelbke, C.; Prodehl, C.: Deep structure of the southern Rhinegraben area from seismic refraction investigations. Z. Geophys. **41**, 333–356, 1975
- Fritsch, J.: Refraktionsseismik. In: Lang, H.D. (ed.): Geologisch-lagerstättenkundliche und geophysikalische Untersuchungen im Siegerländer-Wieder Spateisenbezirk. Beih. geol. Jb. **90**, 90–99, 1971
- Fuchs, K.; Landisman, M.: Results of a re-interpretation of the N-S refraction line Adelebsen-Hilders South in West-Germany. Z. Geophys. **32**, 121–123, 1966a
- Fuchs, K.; Landisman, M.: Detailed crustal investigation along a north-south section through the central part of Western Germany. In: Steinhart, J.S.; Smith, T.J. (eds.): The earth beneath the continents, Geophys. Monogr. **10**, Am. Geophys. Un., Washington, D.C., 433–452, 1966b
- Fuchs, K.; Müller, G.: Computation of synthetic seismograms with the reflectivity method and comparison with observations. Geophys. J. Roy. Astron. Soc. **23**, 417–433, 1971
- German Research Group for Explosion Seismology: Crustal structure in western Germany. Z. Geophys. **30**, 209–234, 1964
- Giese, P.: Results of the generalized interpretation of the deep-seismic sounding data. In: Giese, P.; Prodehl, C.; Stein, A. (eds.): Explosion seismology in western Germany—data and results. Berlin-Heidelberg-New York: Springer 201–214, 1976a
- Giese, P.: The basic features of crustal structure in relation to the main geological units. In: Giese, P.; Prodehl, C.; Stein, A. (eds.): Explosion seismology in central Europe—data and results, Berlin-Heidelberg-New York: Springer 221–242, 1976b
- Giese, P.; Hinz, E.; Prodehl, C.; Schröder, H.; Stein, A.: Description of profiles. In: Giese, P.; Prodehl, C.; Stein, A. (eds.): Explosion seismology in central Europe—data and results. Berlin-Heidelberg-New York: Springer 73–112, 1976
- Giese, P.; Prodehl, C.; Stein, A. (eds.): Explosion seismology in central Europe—data and results. Berlin-Heidelberg-New York: Springer 429 p., 1976
- Giese, P.; Stein, A.: Versuch einer einheitlichen Auswertung tiefenseismischer Messungen aus dem Bereich zwischen der Nordsee und den Alpen. Z. Geophys. **37**, 237–272, 1971
- Glocke, A.: Refraktions- und reflexionsseismische Untersuchungen zur Erforschung der Struktur der Erdkruste im Rhein-Main Gebiet, Versuch einer Gesamtdarstellung. Diplomarbeit, Univ. Frankfurt, 1970
- Glocke, A.; Meissner, R.: Near-vertical reflections recorded at the wide-angle profile in the Rhenish Massif. In: Giese, P.; Prodehl, C.; Stein, A. (eds.): Explosion seismology in central Europe—data and results, Berlin-Heidelberg-New York: Springer 252–256, 1976
- Hänel, R.: Ergänzungsmessungen auf dem Profil zwischen Rhön und Hunsrück. In: Mueller S. (ed.): Kurzfassungen der Vorträge des DFG-Kolloquiums "Erforschung des tieferen Untergrundes in Mitteleuropa" in Stuttgart vom 22.–24.4.1963, Universität Stuttgart, 22V5, 2 p., 1963
- Hänel, R.: Ergänzungsmessungen auf einem Profil zwischen Rhön und Ahrgebirge. In: Rosenbach, O. (ed.): Kurzfassungen der Vorträge des DFG-Kolloquiums "Erforschung des tieferen Untergrundes in Mitteleuropa", in Bad Kreuznach vom 9.–12.3.1964, Universität Mainz, 9N5, 2 p., 1964

- Henningsen, D.: Einführung in die Geologie der Bundesrepublik Deutschland. Stuttgart: Enke-Verlag, dtv, Wiss. Reihe 4182. 119 p., 1976
- Hirn, A.; Perrier, G.: Deep seismic sounding in the Limagne graben. In: Illies, H.; Fuchs, K. (eds.): Approaches to taphrogenesis, Stuttgart: Schweizerbart, 329–340, 1974
- Hoyer, P.; Clausen, C.D.; Leuteritz, K.; Teichmüller, R.; Thome, K.N.: Ein Inkohlungsprofil zwischen dem Gelsenkirchener Sattel des Ruhrkohlenbeckens und dem Ostsauerländer Hauptsattel. Fortschr. Geol. Rheinld. u. Westf. **24**, 161–172, 1974
- Meißner, R.; Bartelsen, H.; Glocke, A.; Kaminski, W.: An interpretation of wide angle measurements in the Rhenish Massif. In: Giese, P., Prodehl, C.; Stein, A. (eds.): Explosion seismology in central Europe – data and results. Berlin-Heidelberg-New York: Springer 245–251, 1976a
- Meißner, R.; Berckhemer, H.: Seismic refraction measurements in the northern Rhinegraben. In: Rothé, J.P.; Sauer, K. (eds.): The Rhinegraben Progress Report 1967. Abh. Geol. Landesamt Baden-Württemberg **6**, 105–108, 1967
- Meißner, R.; Berckhemer, H.; Glocke, A.: Results from deep seismic sounding in the Rhine-Main-area. In: Giese, P.; Prodehl, C.; Stein, A. (eds.): Explosion seismology in central Europe – data and results, Berlin-Heidelberg-New York: Springer 303–312, 1976b
- Meißner, R.; Berckhemer, H.; Wilde, R.; Poursadeg, M.: Interpretation of seismic refraction measurements in the northern part of the Rhinegraben. In: Illies, H., Mueller, S. (eds.): Graben problems, Stuttgart: Schweizerbart, 184–190, 1970
- Meißner, R.; Vetter, U.: The northern end of the Rhinegraben due to some geophysical measurements. In: Illies, H.; Fuchs, K. (eds.): Approaches to taphrogenesis, Stuttgart: Schweizerbart, 236–243, 1974
- Mooney, W.D.; Prodehl, C.: Crustal and upper-mantle structure in the Rhenohercynian zone of western Germany. Abstract, EOS **58**, 912, 1977
- Müller, G.; Fuchs, K.: Inversion of seismic records with the aid of synthetic seismograms. In: Giese, P.; Prodehl, C.; Stein, A. (eds.): Explosion seismology in central Europe – data and results. Berlin-Heidelberg-New York: Springer 178–188, 1976
- Mueller, S.; Peterschmitt, E.; Fuchs, K.; Emter, D.; Ansoerge, J.: Crustal structure of the Rhinegraben area. In: Mueller, S. (ed.): The structure of the earth's crust based on seismic data. Tectonophysics **20**, 381–392, 1973
- Perrier, G.; Ruegg, J.C.: Structure profonde du Massif Central français. Ann. Géophys. **29**, 435–502, 1973
- Plaumann, S.: Bericht über die Auswertung des refraktionsseismischen Profils Adelebsen. In: Niedersächsisches Landesamt für Bodenforschung (ed.): Kurzfassungen der Vorträge des DFG-Kolloquiums "Erforschung des tieferen Untergrundes in Mitteleuropa" in Frankfurt vom 4.–6.1.1961, NLFH Hannover, 5 p., 1961a
- Plaumann, S.: Bericht über die Auswertung des seismischen Profils Kirchheimbolanden. In: Niedersächsisches Landesamt für Bodenforschung (ed.): Kurzfassungen der Vorträge des DFG-Kolloquiums "Erforschung des tieferen Untergrundes in Mitteleuropa" in Frankfurt vom 4.–6.1.1961, NLFH Hannover, 9 p., 1961b
- Prodehl, C., Ansoerge, J., Edel, J.B.; Emter, D., Fuchs, K., Mueller, S.; Peterschmitt, E.: Explosion seismology in the central and southern Rhinegraben – a case history. In: Giese, P.; Prodehl, C., Stein, A. (eds.): Explosion seismology in central Europe – data and results. Berlin-Heidelberg-New York: Springer 313–328, 1976
- Rhinegraben Research Group for Explosion Seismology: The 1972 seismic refraction experiment in the Rhinegraben. – First results. In: Illies, H.; Fuchs, K. (eds.): Approaches to taphrogenesis, Stuttgart: Schweizerbart, 122–137, 1974
- Stein, A.: Ein Gegenschußprofil Kellerwald-Bayrischer Wald. In: Mueller, S. (ed.): Kurzfassungen der Vorträge des DFG-Kolloquiums "Erforschung des tieferen Untergrundes in Mitteleuropa" in Stuttgart vom 22.–24.4.1963, Universität Stuttgart, 22V4, 2 p., 1963
- Stein, A.: Some results of deep seismic sounding in the Rhenish Massif. Report at 33rd JLG Meeting of Working Party on Geodynamics at Walferdange, Luxembourg, May 1977
- Strobach, K.: Ein Gegenschußprofil von der Rhön zum Odenwald. In: Mueller, S. (ed.): Kurzfassungen der Vorträge des DFG-Kolloquiums "Erforschung des tieferen Untergrundes in Mitteleuropa" in Stuttgart vom 22.–24.4.1963, Universität Stuttgart, 22V6, 4 p., 1963

- Thyssen, F.; Allnoch, H.G.; Lüttkebohmer, G.. Einige Ergebnisse geophysikalischer Arbeiten im Bereich der Bramschen Anomalie. *Fortschr. Geol. Rheinld. und Westf.* **18**, 395–410, 1971
- Wangemann, E.-K.. Die Geschwindigkeitsverteilung in der Erdkruste im Gebiet des Süddeutschen Dreiecks, abgeleitet aus refraktionsseismischen Messungen auf einem gestaffelten Nord-Süd-Profil, Diplomarbeit, Univ. Hamburg, 73 p., 1970
- Weber, V.: Zusammenhang zwischen Laufzeit und Form refraktionsseismischer Signale am Beispiel des Profils 20-070 (Birresborn). Diplomarbeit, Techn. Univ. Clausthal, 68 p., 1970
- Wilde, R.: Refraktionsseismische Untersuchungen auf dem Kraichgauprofil. Diplomarbeit, Univ. Frankfurt/Main., 1969

Received April 24, 1978 / Revised version July 10, 1978

